ON-LINE SUPPORTING INFORMATION

Inhaled Nanoparticles Accumulate At Sites Of Vascular Disease

Mark R. Miller[1†]* and Jennifer B. Raftis,[2†] Jeremy P. Langrish,[1] Steven G. McLean,[1] Pawitrabhorn Samutrtai,[3] Shea P. Connell,[1] Simon Wilson,[1] Alex T. Vesey,[1] Paul H.B. Fokkens,[4] A. John F. Boere,[4] Petra Krystek,[5] Colin J. Campbell,[3] Patrick W.F. Hadoke,[1] Ken Donaldson,[2] Flemming R. Cassee,[4,6] David E. Newby,[1] Rodger Duffin[2#] and Nicholas L. Mills[1#]

[1] BHF Centre for Cardiovascular Science, University of Edinburgh, Edinburgh, United Kingdom
[2] MRC Centre for Inflammation Research, University of Edinburgh, Edinburgh, United Kingdom
[3] EaStCHEM School of Chemistry, University of Edinburgh, Edinburgh, United Kingdom
[4] National Institute for Public Health and the Environment (RIVM), Bilthoven, The Netherlands
[5] Institute for Environmental Studies (IVM), VU University, Amsterdam, The Netherlands
[6] Institute for Risk Assessment Sciences, Utrecht University, Utrecht, The Netherlands

[†] Joint and equal contribution to first authorship
[#] Joint and equal contribution to senior authorship

***Correspondence and requests for reprints**
Dr Mark Miller
University/BHF Centre for Cardiovascular Science
University of Edinburgh
Queens Medical Research Institute
47 Little France Crescent
Edinburgh, EH16 4TJ
United Kingdom
Tel: +44 131 242 9334
Fax: +44 131 242 9215
Email: mark.miller@ed.ac.uk

- **Supplementary Tables S1-S4**
- **Supplementary Figures S1-S4**
- **Methods in Full**

Supplementary Table S1. Baseline characteristics of healthy volunteers participating in single size (5 nm) gold exposure study

Parameter	All subjects (n=14)
Age, years	22 (19 – 34)
Height, cm	180 ± 4
Weight, kg	79 ± 11
Body Mass Index, kg/m^2	24.3 ± 2.7
Body Surface Area, m^2	2.76 ± 1.28
FEV_1, L	4.7 ± 0.4
Vital capacity, L	5.6 ± 0.5
Systolic blood pressure, mmHg	130 ± 12
Diastolic blood pressure, mmHg	74 ± 10
Heart rate, bpm	74 ± 15

Data expressed as mean ± standard deviation or median (range) as appropriate. FEV_1 = forced expiratory volume in 1 second. Body surface area calculated using the Mosteller formula[1].

Supplementary Table S2. Baseline characteristics of healthy volunteers participating in size comparison (5 *vs* 30 nm) gold nanoparticle exposure study

Parameter	Small particle exposures (n=10)	Large particle exposures (n=9)
Age, years	28 ± 13	22 ± 4
Height, cm	177 ± 5	178 ± 9
Weight, kg	74 ± 11	79 ± 13
Body Mass Index, kg/m^2	24 ± 3	25 ± 3
Heart rate, bpm	70 ± 9	75 ± 15
Systolic blood pressure, mmHg	131 ± 7	145 ± 15
Diastolic blood pressure, mmHg	75 ± 9	79 ± 9

Data expressed as mean ± standard deviation

Supplementary Table S3. Baseline characteristics of carotid endarterectomy patients

Parameter	Controls (n = 10)	Gold exposed (n=3)
Age, years	72 (62 – 76)	69 (56 – 79)
Sex, men (%)	7 (70)	2 (67)
Height, cm	165 ± 10	169 ± 1
Weight, kg	73 ±12	93 [92 – 112.6]
Body Mass Index, kg/m^2	27.0 ± 4.4	32 [32 – 40]
Systolic Blood Pressure, mmHg	151 ± 22	147 ± 18
Diastolic Blood Pressure, mmHg	81 ± 13	78 ± 7
Creatinine, µmol/L	82.7 ± 28.7	75.7 ± 11.1

Data expressed as mean ± standard deviation, mean (range) or median [interquartile range] as appropriate.

Supplementary Table S4. Levels of gold in reference samples for HR-ICPMS

Reference sample (Lot number)	SEROnorm concentrations	Laboratory concentrations
Sample 1 (201605; 503109)	0.022±0.003 ng/mL	0.017±0.005 ng/mL
Sample 2 (201205; 1003192)	0.007±0.002 ng/mL	0.009±0.006 ng/mL

Data expressed as mean ± standard deviation

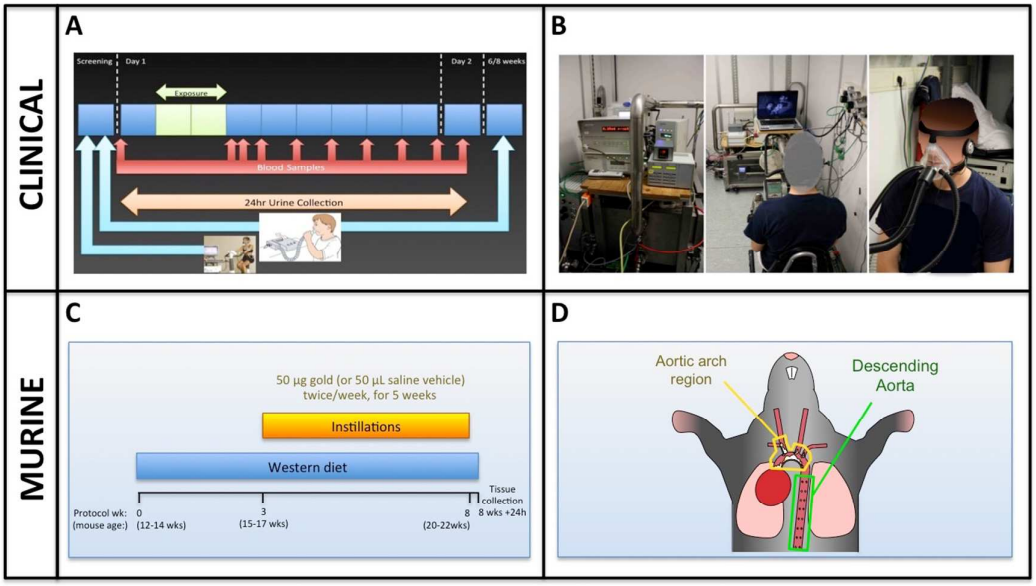

Supplementary Figure S1. Experimental design. **(A)** Protocol and sampling procedure for the gold nanoparticle inhalation studies in man. **(B)** Exposure monitoring equipment and volunteer wearing inhalation apparatus. Image has been modified to protect the identity of the volunteer. **(C)** Feeding and instillation protocol for experiments with gold nanoparticle-treated apolipoprotein E knockout mice. **(D)** Regions of the vasculature selected to investigate the vascular uptake of translocated nanoparticles in atherosclerotic (aortic arch region) and non-atherosclerotic (descending aorta) arteries from mice using the 8-week feeding regime.

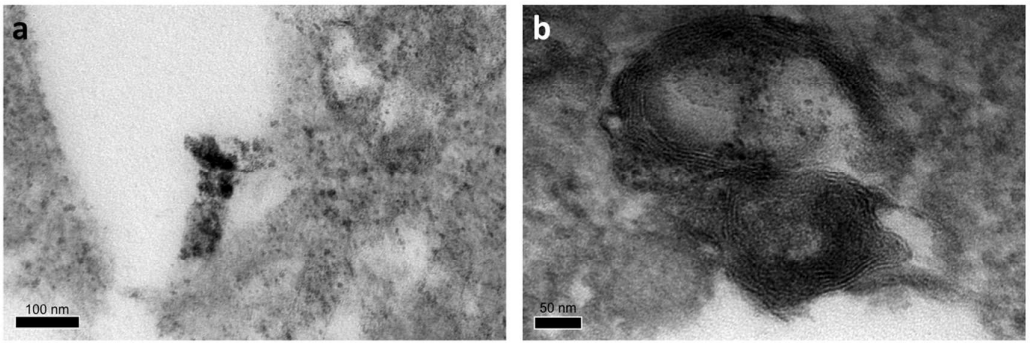

Supplementary Figure S2. Use of transmission electron microscopy to visual translocated gold nanoparticle within atherosclerotic plaques. **(A)** Granular electron-dense particle clusters were evident in some section of tissue from the lipid-rich areas of plaques. **(B)** Other electron dense structures were also seen in the plaques of both saline- and gold-treated animals. However, these regions had a layered structure likely representing calcium bound to lipid droplets or membranous segments from necrotic cell nuclei.

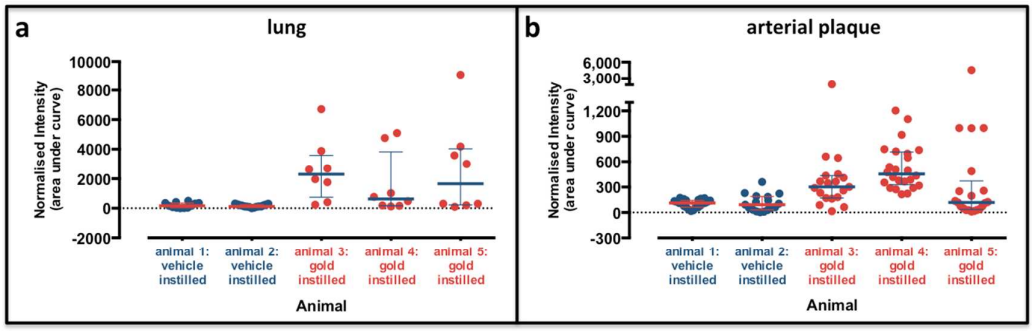

Supplementary Figure S3. Raman spectroscopy consistently confirms the presence of particulate gold in tissue sections of gold-treated animals**.** Characteristic spectra of gold-silver conjugates (see main manuscript) were observed in the **(A)** lung and **(B)** atherosclerotic plaques in different gold-instilled animals, but not in saline-instilled animals, using a subset of tissues from 5 different animals.

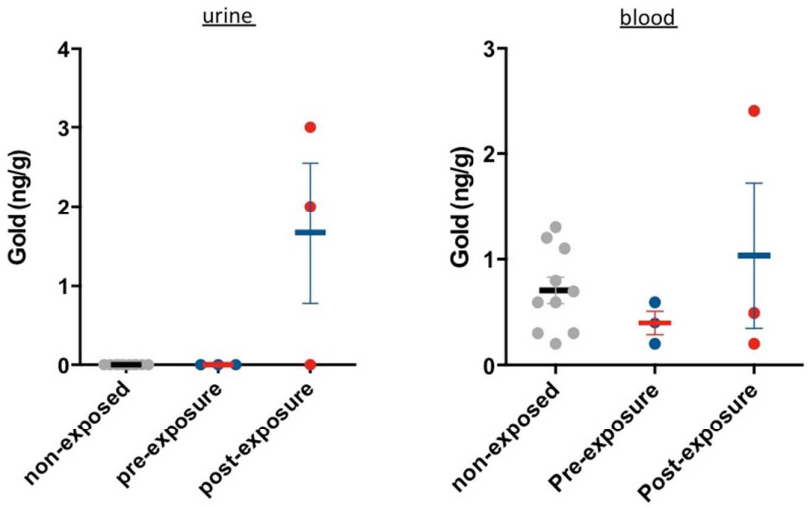

Supplementary Figure S4. HR-ICPMS measurement of gold in the urine and blood of endarterectomy patients. Data expressed as mean ± S.E.M. (n=10 non-exposed, n=3 gold-exposed).

Methods in Full

Gold nanoparticles

In clinical studies, gold nanoparticles (~5nm primary diameter) were freshly generated from gold electrodes (3-4 mm thick, 6mm diameter) using a commercial spark generator operated at a fixed spark frequency (Palas CFG1000, Palas GmbH, Karlsruhe, Germany) in an atmosphere of pure argon, prior to dilution in filtered and conditioned air for exposures. Larger gold nanoparticles for clinical inhalation studies were generated by extending the residence time in argon *via* a through a growth loop, consisting of coiled tubing and buffers, allowing particles to agglomerate by coagulation. The agglomerates were subsequently fused into spherical gold particles of about 30 nm primary diameter by passing the gold aerosol through an oven heated to 600^{o}C, before being diluted in filtered air, which resulted in solid spherical single particles. Exposure was monitored in real time for particle number concentration (CPC 3022, TSI Inc., St Paul, USA), surface area (NSAM 3550, TSI Inc., St Paul, USA) and size distribution (SMPS 3080, TSI Inc., St Paul, USA). Samples were collected onto two parallel Teflon filters (R2PJ047, Pall Corp., Ann Arbor, USA) and gravimetrically analyzed for particle mass concentration. Primary particle size in the resulting suspension was determined by transmission electron microscopy (TEM; Phillips CM120 Transmission electron microscope; FEI UK Ltd, Cambridge, UK) and atomic force microscopy (AFM; XE-100 AFM, Park Systems Corp., Korea)[2].

Gold nanoparticle suspensions used for the murine study were purchased from BBInternational (Cardiff, UK). TEM (Phillips CM120; FEI UK Ltd) was used to confirm the primary particle size. Mean particle size in suspension was determined by dynamic light scattering to ensure there was minimal agglomeration of gold particles prior to instillation. Suspensions were diluted 100-fold in PBS (BBInternational) and particle size measured using a PS90 Particle Size Analyzer (Brookehaven Instrument Corporation, New York, USA) set to the following parameters: 37^{o}C, angle 90^{o}; run duration 1 min; refractive index of particles 0.2 ‘real’ (0 ‘imaginary’); dust cut-off 30.

Clinical Studies

All subjects gave their written informed consent, and the studies were reviewed and approved by the local research ethics committee according with the Declaration of Helsinki.

Healthy volunteer studies

Healthy male non-smoking volunteers aged 18-35 (**Supplementary Tables S1** & **S2**) were recruited from the University of Edinburgh. Subjects taking regular medication and those with clinical evidence of atherosclerotic vascular disease, arrhythmias, diabetes mellitus, hypertension, renal or hepatic failure, asthma, significant occupational exposure to air pollution, or an intercurrent illness likely to be associated with inflammation were excluded from the study. Subjects had normal lung function and reported no symptoms of respiratory tract infection for at least 6 weeks before or during the study. All subjects abstained from alcohol for 24 hours and from food, tobacco, and caffeine-containing drinks.

Healthy subjects attended for a screening visit where lung function was performed (Vitalograph, Buckingham, UK) and a cardiopulmonary exercise carried out to confirm the workload needed to generate an average minute ventilation of 25 L/min/m^2 body surface area. Subjects were exposed to the gold aerosol for 2 hours during intermittent exercise on a recumbent exercise bicycle (Heinz-Kettler GmbH, Ense-Parsit, Germany) at the predefined workload, in a specially built human controlled exposure chamber. The output of the nanoparticle generator was mixed with HEPA filtered air at 80 L/min, stabilized in a 200 L mixing chamber (residence time ~2.5 min) and delivered to the subject through a facemask (ComfortFull 2, Philips Healthcare, Best, Netherlands) (**Supplementary Figure S1A** & **S1B**). Following exposure, volunteers were taken to the adjacent clinical research facility, for sample collection were carried out in a quiet, temperature-controlled room maintained at 22°C to 24°C with subjects lying supine. Subjects remained indoors during this time to minimize additional exposure to particulate air pollution.

Carotid endarterectomy studies

Patients presenting to the Lothian Stroke services with a recent acute cerebrovascular syndrome (transient ischaemic attack, amaurosis fugax or stroke) and scheduled for carotid endarterectomy were recruited (**Supplementary Table S3**). Exclusion criteria were: recent body-piercing or history of gold tooth filling, psychiatric illness/social situations that would limit compliance with study requirements, patients with new stroke and a modified Rankin score >3, pregnant women, participation in the study would result in delay to carotid surgery, history of allergic reaction attributed to elemental gold or molecules including gold. The study followed an accepter/rejecter model (*i.e.* patients who didn't consent to gold inhalation, could be included as controls – a randomized model was not felt to be feasible given the significant scheduling challenges in these acutely unwell patients who require surgery as soon as possible).

Gold exposed patients inhaled gold nanoparticles (~5 nm diameter) on the day prior to surgery, as described above. Patients were not exercised during exposure (to minimize the risk of mechanical stress on a fragile and acute plaque), thus, the duration of exposure was increased to two periods of 2-h (first in morning, the second in the afternoon) to maximize particle exposure. Blood and urine samples were taken prior to gold exposure and at the time of surgery. For control patients blood and urine samples were only taken at the time of surgery. At surgery, the plaque was excised intact as part of a standard carotid endarterectomy and patch angioplasty. The plaque was immediately handed off table, oriented and photographed. The specimen was then snap frozen in liquid nitrogen and transferred to a freezer for subsequent batch analysis.

Blood and urine sampling

Blood samples were obtained through an in-dwelling intravenous cannula before and after gold exposure and at predefined intervals (**Supplementary Figure S1A**). Samples were collected into Lithium Heparin (S-Monovette® for trace metal analysis, Sarstedt AG, Nümbrecht, Germany) before being transferred to disposable soda lime digestion tubes

(Duran Group, Mainz, Germany) and stored at -20°C before further analysis. Urine was collected over 24 hours following exposure. Total urine was thoroughly mixed and subsamples were separated into aliquots and frozen at -40°C until further analysis. Blood samples collected before and 24 hours after exposure to gold nanoparticles, as well as later time points in some studies, and were analysed in the regional hematology and clinical chemistry reference laboratory.

Animal Studies

All experiments were performed according to the Animals (Scientific Procedures) Act 1986 (UK Home Office).

Animals and exposures

Male apolipoprotein E knockout ($ApoE^{-/-}$) mice ($Apoe^{tm1Unc}$/J; Charles River UK; n=8/group) aged 12-14 weeks at the start of the protocol were fed a high-fat "Western diet" (Research Diets, New Brunswick, USA) for 8 weeks[3]. Gold nanoparticles (citrate-coated, primary particle size 5nm; BBInternational, UK) in suspension (50 µL of 2.3 mg/mL), or vehicle, were sonicated for 20 min then administered to the lungs of mice by instillation twice weekly for the last 5 weeks of feeding (**Supplementary Figure S1C**). In experiments exploring particle size, 2, 5, 10, 30 or 200 nm particles (BBInternational) were used as above, with the exception that a stock solutions were diluted in order that all sizes were of an equivalent mass concentration (0.8 mg/mL).

Animals were euthanized ~18 hours after the last instillation. Blood samples from the vena cava and liver biopsies were taken, and stored in soda lime digestion tubes at -80°C. The lungs were cannulated via a small incision in the trachea and lavaged 3 times with 0.8 mL sterile saline to collect bronchoalveolar lavage fluid (BALF). BALF was centrifuged at 180*g* for 5 min at 4°C, the supernatant was removed, and the cell pellets combined. Cell pellets were resuspended in 1 mL of phosphate-buffered saline (PBS) and total cell numbers were counted using an automatic cell counter (Satorius Steadman, Chemometec, Nucleocounter®,

Gydevang, Denmark). The aortic arch (and immediate branches: ~8 mm of brachiocephalic, left carotid and left subclavian arteries) and descending thoracic aorta (from end of curvature of arch to intersection with diaphragm) were cleaned of perivascular fat, rinsed in saline, blotted dry and frozen at -80^{o}C in digestion tubes. The aortic arch region is used as an area of vasculature with extensive atherosclerotic lesions of a mixed 'complex' plaque phenotype[4], whereas the descending aorta is largely free of atherosclerotic plaques in mice at this end under this feeding regime (**Supplementary Figure S1D**)[3]. Sample weight was determined by comparison of tubes weights before and after collection of the sample.

Quantification of Gold in Biological Samples using HR-ICPMS

Biological samples were completely dissolved in aqua regia (0.5 mL 60% HNO_3 and 1.5 mL 30% HCl; 120^{o}C) and diluted with ultrapure water to a final volume of 10 mL before analysis for gold content using high resolution inductively coupled plasma mass spectroscopy (HR-ICPMS; Element XR, Thermo Fisher, Bremen, Germany)[5, 6]. Urine samples were directly diluted with aqua regia by a factor of 10 and analysed afterwards by HR-ICPMS. An external calibration curve of the interference-free isotope ^{197}Au was performed in the low-resolution mode between 0 and 40 ng/L. On-line addition and correction with an internal standard (1 µg/L rhodium with the measured isotope ^{103}Rh in the low-resolution mode) and the correction for the chemical blank were applied too. All chemicals used were of analytical grade or of high purity. Nitric acid (HNO_3) and hydrochloric acid (HCl) were purchased from Merck, Darmstadt, Germany. The calibration standard solution of gold (Au), as well as a solution of the element rhodium (Rh) used as internal standard, were prepared using single element stock solutions with a concentration of 1000 mg/mL (both Inorganic Ventures; Instrument Solutions, Nieuwegein, The Netherlands). For quality control aspects on the relevant ultra-trace level, two reference samples "SERONorm Trace levels in blood" (supplied by C.N. Schmidt, Amsterdam, The Netherlands; **Supplementary Table S4**) were analyzed, using two different batch numbers. The methodological limit of quantification was 0.03 ng/gram of blood, and the coefficient of variation was 5.5% for blood samples run in triplicate.

Histology and electron microscopy

Additional animals (3 gold-instilled, 2 vehicle-instilled) were used to provide arterial (brachiocephalic) and pulmonary tissue for histology and electron microscopy. The lungs of these animals were not lavaged and were instead perfusion fixed with ~2 mL of methacarn fixative (60% methanol, 30% chloroform and 10% glacial acetic acid) and the lungs allowed to slowly inflate under gravity. Arterial and liver samples were fixed overnight in 10% neutral-buffered formalin before being transferred to 50% ethanol until time of analysis. Samples were embedded in paraffin, 5 μm thick sections prepared, and then stained with hematoxylin and eosin (lung) or United States Trichrome (arteries).

Samples of the aortic arch for transmission electron microscopy (TEM) were fixed for 2-h in 3% glutaraldehyde (in 0.1 M sodium cacodylate buffer, pH 7.3) and post-fixed for 45 min in 1% osmium tetroxide (in 0.1 M sodium cacodylate). The samples were then dehydrated in increasing concentrations of acetone before being embedded in Araldite® resin. Sections (1 μm thick) were cut on a Reichert OMU4 ultramicrotome (Leica Microsystems Ltd, Milton Keynes, UK), stained with toluidine blue and viewed in a light microscope to select suitable areas for investigation. Ultrathin sections (60 nm thick) were cut from selected areas, stained in uranyl acetate and lead citrate, then viewed in a Phillips CM120 Transmission electron microscope (FEI UK Ltd, Cambridge, UK). Images were taken on a Gatan Orius CCD camera (Gatan Oxon, UK).

Silver Staining and Raman Spectroscopy

Raman spectroscopy was performed using unstained histological sections that had been de-paraffinized in graded alcohol. Detection of gold particulate was assisted by conjugation to silver using a LI-silver enhancement kit (Molecular Probes, Invitrogen, Paisley, UK). Tissue sections were incubated in 50 nM glycine in phosphate-buffered saline (PBS pH 7.4; 5 min) to block aldehyde groups in the fixation reagent, then thoroughly rinsed with dH_2O to remove

all traces of phosphate ions from PBS. Silver staining reagents were added for 5 min before washing with water and leaving to air dry.

Detection of gold within tissue samples was performed by Raman spectroscopy (Renishaw inVia, Renishaw UK). The laser was set at 514 nm (based on absorbance spectra from preliminary experiments) with pinhole at 15 mW. Incident light was focused to the samples by 50× Olympus long working distance objective (NA = 0.45) with 2.1 μm focal diameter. Exposure time and laser power used in the determination were varied depending on tissue sections. Raman spectra from the lung tissue sections were collected with exposure time of 60 seconds and 10% laser power. In arterial sections the exposure time of 100 seconds and 50% laser power were used. The charge coupled device (CCD) detector was used with Peltier cooling to -70˚C, using a CCD area of 9,000-11,000 counts. In carotid samples, a rectangular selection of 5,000-6,000 scans was performed to generate a 'heat map' for the localization of spectra positive for gold.

Raman spectra were processed using Wire2.0 software and analyzed using Origin8.0 software. Baselines of all Raman spectra were corrected to a horizontal slope in order to calculate noise intensities. Range of frequency with no Raman signal was used to determine the intensities of noise by taking the average signal + (3x standard deviation). Intensities of signal were calculated by dividing the intensity of signal by the intensity of noise. Spectra were quantified by transforming data to area under the curve (spectra) between a Raman shift of 950 – 1750 cm^{-1}.

Quantification of atherosclerosis

Atherosclerotic burden was comprehensively assessed, as previously described[3]. The aortic arch and descending thoracic aorta was cut longitudinally and lipid-rich atherosclerotic plaques were stained *en-face* using Sudan IV. The coverage of the aortic surface with red-stained plaques was quantified using Image-J software.

The brachiocephalic arteries was selected for histological analysis of plaque burden as this region of artery develops 'complex' fibroelastic plaques that are representative of

human plaque structure[7] and undergo extensive expansion and remodeling during the instillation period of the protocol[8, 9]. Arteries were fixed in formalin and histological sections were taken in triplicate at 100 μm intervals, beginning at the first section of artery with a fully intact media. Sections were stained with United States Trichrome (UST). The cross-sectional area of the plaque was measured and standardised to the area of the vascular media. A single mean value of atherosclerotic burden for each animal was calculated from the plaque size from each complete serial section throughout the brachiocephalic artery. The carotid artery bifurcation was used for quantify atherosclerotic burden in gold-treated animals as brachiocephalic arteries were used for detection of gold by ICMPS.

Plaque structural complexity was assessed by counting distinct adjoining or overlying plaques within each section[10]. Quantitative measurement of plaque constituents was performed using single UST-stained sections from the region of maximal plaque growth. Images of sections were imported into Adobe Photoshop v11.0, and a colour range was selected from three randomly chosen positively stained sections, which was then used to identify positively stained plaque components from all subsequent slides.

Data Analysis

For parametric data (Gaussian distribution) values reported are mean±SEM with differences between groups analyzed by analysis of variance (ANOVA) with Bonferroni post-hoc tests, and Student's *t*-tests, where appropriate (GraphPad Prism v6.0a). For non-parametric (non-normally distributed) data values are reported as median ± interquartile range, with differences between groups analyzed by Kruskal-Wallis followed by Dunn's post-hoc tests, and Mann-Whitney tests. ROUT's outlier[11] (Q=1%, GraphPad Prism v6.0a) was used to detect the presence of outliers in conditions where normalization to very small tissue weights (aortic arch and descending aorta) skewed data sets. $P<0.05$ was taken as statistically significant.

References for Supplementary Material

(1) Mosteller R.D., Simplified calculation of body-surface area. *N. Engl. J. Med.* **1987**, *317*, 1098.

(2) Baalousha M.; Lead J.R., Rationalizing nanomaterial sizes measured by atomic force microscopy, flow field-flow fractionation, and dynamic light scattering: sample preparation, polydispersity, and particle structure. *Environ. Sci. Technol.* **2012**, *46*, 6134-6142.

(3) Miller M.R.; McLean S.G.; Duffin R.; Lawal A.O.; Araujo J.A.; Shaw C.A.; Mills N.L.; Donaldson K.; Newby D.E.; Hadoke P.W., Diesel exhaust particulate increases the size and complexity of lesions in atherosclerotic mice. *Part. Fibre Toxicol.* **2013**, *10*, 61.

(4) Rosenfeld M.E.; Polinsky P.; Virmani R.; Kauser K.; Rubanyi G.; Schwartz S.M., Advanced atherosclerotic lesions in the innominate artery of the ApoE knockout mouse. *Arterioscler. Thromb. Vasc. Biol*. **2000**, *20*, 2587-2592.

(5) Krystek P.; Ritsema R., Validation assessment about the determination of selected elements in groundwater by high-resolution inductively coupled plasma mass spectrometry (HR-ICPMS). *Int. J. Environ. Analyt. Chem.* **2009**, *89*, 331-345.

(6) Lankveld D.P.; Rayavarapu R.G.; Krystek P.; Oomen A.G.; Verharen H.W.; van Leeuwen T.G.; De Jong W.H.; Manohar S., Blood clearance and tissue distribution of PEGylated and non-PEGylated gold nanorods after intravenous administration in rats. *Nanomedicine (Lond)* **2011**, *6*, 339-349.

(7) Rosenfeld M.E.; Averill M.M.; Bennett B.J.; Schwartz S.M., Progression and disruption of advanced atherosclerotic plaques in murine models. *Curr. Drug Targets* **2008**, *9*, 210-216.

(8) Jackson C.L., Defining and defending murine models of plaque rupture. *Arterioscler. Thromb. Vasc. Biol.* **2007**, *27*, 973-977.

(9) Johnson J.; Carson K.; Williams H.; Karanam S.; Newby A.; Angelini G.; George S.; Jackson C., Plaque rupture after short periods of fat feeding in the apolipoprotein E-knockout mouse: model characterization and effects of pravastatin treatment. *Circulation* **2005**, *111*, 1422-1430.

(10) Cassee F.R.; Campbell A.; Boere A.J.; McLean S.G.; Duffin R.; Krystek P.; Gosens I.; Miller M.R., The biological effects of subacute inhalation of diesel exhaust following addition of cerium oxide nanoparticles in atherosclerosis-prone mice. *Environ. Res.* **2012**, *115*, 1-10.

(11) Motulsky H.J.; Brown R.E., Detecting outliers when fitting data with nonlinear regression - a new method based on robust nonlinear regression and the false discovery rate. *BMC Bioinformatics* **2006**, *7*, 123.